Journal of Sound and Vibration (2002) **251**(1), 13–38
doi:10.1006/jsvi.2001.3978, available online at http://www.idealibrary.com on IDEAL®

SIMPLIFIED MODELS FOR THE LOCATION OF CRACKS IN BEAM STRUCTURES USING MEASURED VIBRATION DATA

J. K. Sinha†, M. I. Friswell and S. Edwards

Department of Mechanical Engineering, University of Wales Swansea, Singleton Park, Swansea SA2 8PP, Wales, U.K. E-mail: m.i.friswell@swansea.ac.uk

(*Received* 23 *October* 2000, *and in final form* 26 *July* 2001)

A new simplified approach to modelling cracks in beams undergoing transverse vibration is presented. The modelling approach uses Euler–Bernoulli beam elements with small modifications to the local flexibility in the vicinity of cracks. This crack model is then used to estimate the crack locations and sizes, by minimizing the difference between the measured and predicted natural frequencies via model updating. The uniqueness of the approach is that the simplified crack model allows the location and damage extent to be estimated directly. The simplified crack model may also be used to generate training data for pattern recognition approaches to health monitoring. The proposed method has been illustrated using the experimental data on beam examples.

1. INTRODUCTION

Health monitoring of mechanical structures using experimentally measured modal data has been a topic of active research for decades. Most of the approaches use the modal data of a structure before damage occurs as baseline data, and all subsequent tests are compared to it. Any deviation in the modal properties from this baseline data is used to estimate the crack size and location. Doebling *et al.* [1] gave a review of the research on crack and damage detection and location in structures using vibration data. The estimation of crack size and location generally requires a mathematical model (usually a finite element (FE) model) along with experimental modal parameters of the structure. The estimation methods are predominately based on the change in natural frequencies [2–6], the change in mode shapes [7–12] or measured dynamic flexibility [13–15]. Salawu [16] gave a review of research work on crack detection based on the change in natural frequencies. Another class of crack detection methods, also based on the change in modal parameters, uses a different identification approach based on the modification of structural model matrices (such as mass, stiffness and damping matrices) using FE model updating methods [1].

A number of gradient-based FE model updating methods have been discussed by Friswell and Mottershead [17]. Many studies using these methods for structural health monitoring have been reported (for example, references [18–20]). In this paper, the proposed method for the detection of crack size and location uses the gradient-based FE

†Permanent address: Scientific Officer, Vibration Laboratory, Reactor Engineering Division, Bhabha Atomic Research Centre, Mumbai 400 085, India.

0022-460X/02/110013 + 26 $35.00/0

model updating approach, although the application is somewhat different in the present study. Most of the earlier studies identified changes in element stiffnesses, or the system stiffness matrices. These methods only approximate the crack size and location to an element, and hence a very fine FE mesh is required to avoid large errors. The explicit use of the location of a crack as an updating parameter is used in this paper in order to reduce this computational burden and improve the localization accuracy. Sinha and Friswell [21] used a similar concept to estimate support locations and stiffnesses.

Measured natural frequencies of the structure are used to estimate the crack size and location. Problems arise in many structures if natural frequencies alone are used, since the symmetry of the structure means that the damage location is often non-unique. Using mode shape data enables a unique solution to be obtained, although natural frequencies are relatively insensitive to damage. This paper demonstrates the use of the simplified crack model using natural frequency data alone, although the model may also be used with algorithms requiring mode shape, frequency or time data. A sensitivity-based FE model updating technique [17] is used based on a correlated FE model. The method detects a crack by simultaneously updating the position and size of the crack in the FE model through the minimization of the difference between the measured and computed natural frequencies. This cost function is a highly non-linear function with respect to the updating parameters, and an iterative solution is obtained. Such an approach requires the formulation and computation of the sensitivity matrix (first order derivatives) of the cost function with respect to the updating parameters. The shape functions of the beam are used to generate the system stiffness matrix as a continuous function of these updating parameters. Thus, the eigenvalue derivative with respect to the updating parameters may be computed analytically, thus producing a more accurate sensitivity matrix. The major difficulty in using a model updating approach is differentiating between damage and any modelling errors that are present in the undamaged structure [22]. There are two approaches to overcome this problem, although both require measurements from the undamaged structure. The first is to update the model of the undamaged structure to obtain a validated model. Care must be taken to ensure that the parameters of the updated model have physical meaning, rather than merely improving the correlation of the measured and predicted data. The second approach considers the changes in frequency between the damaged and undamaged structures, so that to first order the modelling errors are eliminated. Neither approach is able to satisfactorily cope with environmental effects, for example changing temperatures or humidity.

The alternatives to the inverse approach, based on an FE model of the structure, are pattern recognition and signal processing techniques (for example, references [23–26]). These methods determine whether or not damage has occurred, based on *feature vectors* which encode the important dynamic properties of the structure. Localization is usually performed by determining which of a candidate set of sub-structures is damaged. The methods still have problems when the dynamics change due to environmental effects, unless these effects are explicitly incorporated into the feature vectors. Often pattern recognition procedures require a significant number of training data sets that are representative of undamaged and damaged scenarios, and the only realistic source of these data is simulation. The simplified model presented in this paper may also be used to supply training data for pattern recognition algorithms.

There are a number of approaches to the modelling of cracks in beam-type structures reported in the literature. Dimarogonas [27] and Ostachowicz and Krawczuk [28] gave comprehensive surveys of crack modelling approaches. The simplest method for an FE model is to use a reduced stiffness for a complete element to simulate a small crack in that element [8, 11, 13, 29, 30]. Another simple approach is to divide the beam-type structure

into two parts that are pinned at the crack location and the crack is simulated by the addition of a rotational spring [12, 31–33]. These approaches are a gross simplification of the crack dynamics and do not involve the crack size and location directly. The alternative is to model the dynamics close to the crack more accurately, for example producing a closed-form solution giving the natural frequencies and mode shapes of cracked beam directly [34] or using differential equations with compatible boundary conditions satisfying the crack conditions [35–37]. Alternatively, two- or three-dimensional finite element meshes for beam-type structures with a crack may be used [38–40]. These methods produce detailed and accurate FE models but are a complicated and computational intensive approach for modelling simple structures like beams. Furthermore, the FE models will contain modelling errors, the data will include measurement errors, and the use of low-frequency vibration will tend to average out localized effects. The result is that these very detailed models do not substantially improve the results from crack detection and location algorithms. Lee and Chung [41] generated the flexibility matrix of a beam element with a crack using an energy method. Most of the work was theoretical, although some experimental validation has been performed either by using the ratios of the lower natural frequencies or by direct comparison [33, 41].

The model described in this paper is for an open crack. A breathing crack, which opens and closes, produces interesting and complicated non-linear dynamics. Brandon [42] and Kisa and Brandon [43] gave an overview of some of the techniques that may be applied. Many techniques to analyze the resulting non-linear dynamics are based on approximating the bilinear stiffness when the crack opens and closes. The approach proposed in this paper is able to approximate the stiffness matrix for the beam with an open crack. Such an approach will certainly be more efficient than those based on 2-D or 3-D FE models for time integration of the equations of motion. However, any realistic multi-degree-of-freedom non-linear analysis would have to be based on a reduced order model of the structure.

This paper models beam structures with cracks at different locations by using Euler–Bernoulli beam elements with some modification to the local flexibility in the vicinity of the crack. The modelling approach is based on the concept of Christides and Barr [44] and utilizes a simple approximation to the stiffness reduction. Other authors have used similar approaches [45–47]. The formulation is simpler than the method of Lee and Chung [41], and has the advantage that it involves the crack location and depth directly. The modelling of the crack will be discussed first, followed by the incorporation of the crack model into the FE model of the structure and the estimation of the crack location and size from the measured modal data. Experimental results are then used to validate the crack model and also compare the results with those from other crack models. This comparison is intended to show that the proposed crack model is able to give an accuracy similar to other models, but is simpler to apply in health monitoring applications. Finally, the proposed method is demonstrated using experimental examples.

2. THEORY

The problem considered here is a simple beam with multiple cracks along its length, and is shown schematically in Figure 1. It is assumed that the cracks have a uniform depth across the width of the beam, and that they do not change the beam mass. Only fully open cracks are considered. First, the model of the crack will be introduced; this model is then incorporated into the FE model and finally, the estimation of the crack depth and location will be discussed.

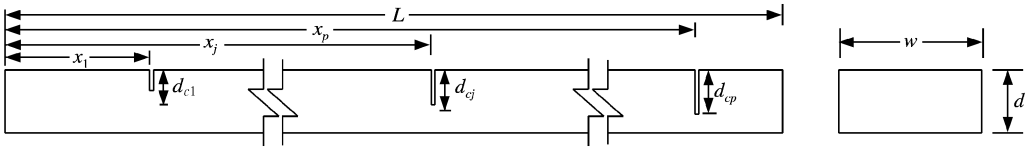

Figure 1. The beam with multiple cracks.

2.1. CRACK MODELLING

Clearly, some of the materials adjacent to the crack will not be stressed and thus will offer only a limited contribution to the stiffness. The actual form of this increased flexibility is quite complicated, but in this paper this phenomenon is approximated by a variation in the local flexibility (EI). In reality, for a crack on one side of a beam, the neutral axis will change in the vicinity of the crack, but this will not be considered here. Christides and Barr [44] considered the effect of a crack in a continuous beam and calculated the stiffness, EI, for a rectangular beam to involve an exponential function given by

$$EI(x) = \frac{EI_0}{1 + C\exp(-2\alpha|x - x_j|/d)}, \tag{1}$$

where $C = (I_0 - I_{cj})/I_{cj}$, $I_0 = wd^3/12$ and $I_{cj} = w(d - d_{cj})^3/12$ are the second moment of areas of the undamaged beam and at the jth crack. w and d are the width and depth of the undamaged beam, and d_{cj} is the crack depth. x is the position along the beam and x_j the position of the crack. α is a constant that Christides and Barr estimated from experiments to be 0·667. The inclusion of the stiffness reduction of Christides and Barr [44] in an FE model of a structure is complicated because the flexibility is not local to one or two elements, and thus the integration required to produce the stiffness matrix for the beam would have to be performed numerically every time the crack position changed. Furthermore, for complex structures, without uniform long beams, equation (1) would only be approximate. The comparison of the proposed model with that of Christides and Barr is intended to show the similarities of the current simplified approach with an established model.

Figure 2 shows the variation of EI for a crack 25% of the beam depth using equation (1). What is clear is that most of the flexibility is local to the crack, although there are also very small changes in flexibility far away from the crack. In this paper, a simplified form of the stiffness variation is used, where the flexibility varies linearly from the uncracked to cracked beam section, as shown in Figure 2. The variation in EI starts from an effective length, l_c, on either side of the crack location, and at the position of highest flexibility the stiffness is the second moment of area of the cracked section and is based on the crack depth. The determination of the length l_c will be considered later. Although this model will not be accurate at high frequencies, for low-frequency vibration this model will produce a local flexibility that gives a sufficiently accurate equivalent model of the beam with a crack. The great advantage of this approach is simplicity. An alternative simple approach is to reduce the stiffness of a whole element. However, the number of elements must increase to obtain good localization, and estimating the crack depth must be done *a posteriori*. Another simple approach models the crack using a pinned connection and a rotary spring. However, this spring must be introduced at a node and estimating the crack depth is

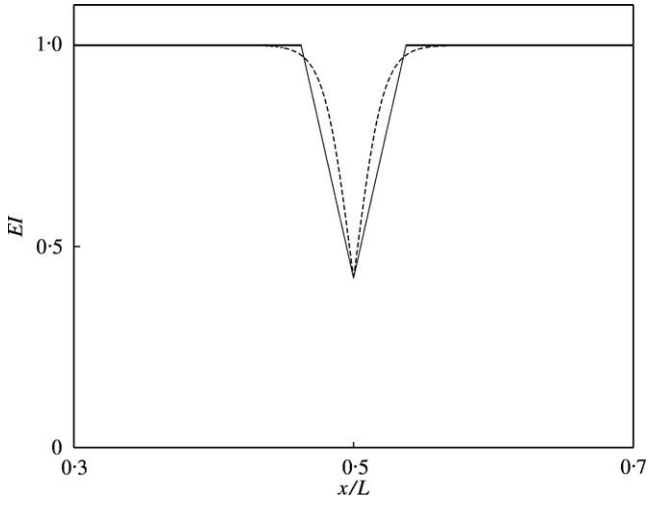

Figure 2. Comparison in the variation in stiffness near a crack for the triangular reduction (solid) and the approach of Christides and Barr [35] (dotted) for a crack depth of 25%.

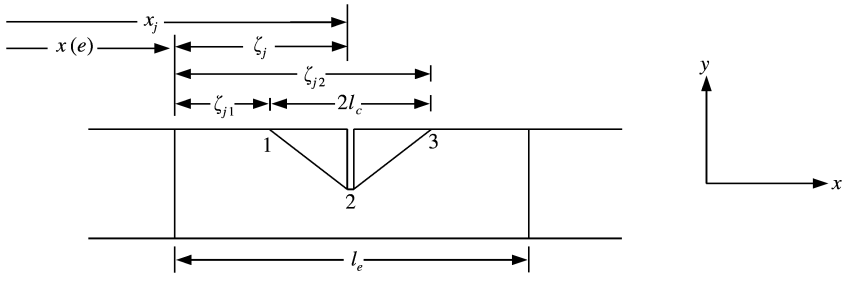

Figure 3. The eth beam element with a triangular variation in stiffness used to model the crack.

difficult. With the triangular reduction in stiffness the crack depth and location are estimated directly.

The flexural rigidity close to the crack, $EI_e(\xi)$, is given by

$$EI_e(\xi) = \begin{cases} EI_0 - E(I_0 - I_{cj})\dfrac{(\xi - \xi_{j1})}{(\xi_j - \xi_{j1})} & \text{if } \xi_{j1} \leqslant \xi \leqslant \xi_j, \\ EI_0 - E(I_0 - I_{cj})\dfrac{(\xi_{j2} - \xi)}{(\xi_{j2} - \xi_j)} & \text{if } \xi_j \leqslant \xi \leqslant \xi_{j2}, \end{cases} \tag{2}$$

where ξ_j is the location of the jth crack within the eth element and $\xi_{j1} = \xi_j - l_c$ and $\xi_{j2} = \xi_j + l_c$ are the positions on either sides of crack where the stiffness reduction begins (see Figure 3).

It remains to determine the effective length of the stiffness reduction for the crack, l_c. One approach is to make the integral of the stiffness reduction in equations (1) and (2) equal. Since most of the flexibility is local in both cases, then for modes where the curvature is

small near the stiffness reduction, ensuring these integrals are equal would produce equal natural frequency changes due to the crack. The integrals are

$$\text{from equation (1)}, \quad \int_{-\infty}^{\infty} [EI_0 - EI(x)]\,\mathrm{d}x = EI_0 \frac{d}{\alpha} \log_e(1 + C) \approx EI_0 \frac{dC}{\alpha},$$

$$\text{from equation (2)}, \quad \int_{\xi_{j1}}^{\xi_{j2}} [EI_0 - EI_e(x)]\,\mathrm{d}\xi = EI_0 l_c \frac{C}{1 + C} \approx EI_0 l_c C, \tag{3}$$

where the approximations are of the first order in C. Thus, a good approximation seems to be

$$l_c = \frac{d}{\alpha} = 1{\cdot}5d, \tag{4}$$

where the value for α estimated by Christides and Barr [44] has been used. The quality of this model will be checked later using the experimental data. Note that this length does not change with the crack depth, but instead depends on the beam depth.

2.2. FINITE ELEMENT MODELLING OF A BEAM WITH A CRACK

The Euler–Bernoulli formulation was used to model the beam and only bending in a single plane is considered. A consistent mass matrix is used. Each node has two degrees of freedom, namely the translational displacement and bending rotation. The cracks are assumed to be placed within the beam elements of the FE model. The derivation of the reduced stiffness due to a single crack will be outlined. Consider the jth crack at location x_j within the eth element of beam, as shown in Figure 3. It will be assumed that the stiffness reduction all falls within a single element. If the stiffness reduction extends over more than one element, then the following approach may be easily extended to include integration over all the elements affected. The alternative is to move the nodes of the model to ensure that the crack effect is contained within a single element.

The stiffness matrix of the eth element of the beam may be written as

$$\mathbf{K}_{e,crack} = \mathbf{K}_e - \mathbf{K}_{cj}, \tag{5}$$

where $\mathbf{K}_e$ is the element stiffness matrix for the eth element with no crack and $\mathbf{K}_{cj}$ is the reduction in the stiffness matrix due to the jth crack. This stiffness reduction, $\mathbf{K}_{cj}$, must be obtained in terms of the crack position and depth. The nodal degrees of freedom, $[w_{e1}\ w_{e2}\ w_{e3}\ w_{e4}]^{\mathrm{T}}$, are ordered in the usual way. The stiffness matrix is obtained using the standard integration based on the variation in flexural rigidity as

$$[\mathbf{K}_{e,crack}]_{rs} = \int_0^{l_e} EI_e(\xi) N''_{er}(\xi) N''_{es}(\xi)\,\mathrm{d}\xi, \tag{6}$$

where the shape functions, $N_{ei}(\xi)$, are those for a standard Euler–Bernoulli beam element, namely,

$$N_{e1}(\xi) = \left(1 - 3\frac{\xi^2}{l_e^2} + 2\frac{\xi^3}{l_e^3}\right), \qquad N_{e2}(\xi) = l_e\left(\frac{\xi}{l_e} - 2\frac{\xi^2}{l_e^2} + \frac{\xi^3}{l_e^3}\right),$$

$$N_{e3}(\xi) = \left(3\frac{\xi^2}{l_e^2} - 2\frac{\xi^3}{l_e^3}\right), \qquad N_{e4}(\xi) = l_e\left(-\frac{\xi^2}{l_e^2} + \frac{\xi^3}{l_e^3}\right). \tag{7}$$

and l_e is the length of the eth element. Using equations (2), (6) and (7), the matrix $\mathbf{K}_{cj}$ is

$$\mathbf{K}_{cj} = \begin{bmatrix} k_{11} & k_{12} & -k_{11} & k_{14} \\ k_{12} & k_{22} & -k_{12} & k_{24} \\ -k_{11} & -k_{12} & k_{11} & -k_{14} \\ k_{14} & k_{24} & -k_{14} & k_{44} \end{bmatrix}, \tag{8}$$

where

$$k_{11} = \frac{12E(I_0 - I_{cj})}{l_e^4}\left[\frac{2l_c^3}{l_e^2} + 3l_c\left(\frac{2\xi_j}{l_e} - 1\right)^2\right],$$

$$k_{12} = \frac{12E(I_0 - I_{cj})}{l_e^3}\left[\frac{l_c^3}{l_e^2} + l_c\left(2 - \frac{7\xi_j}{l_e} + \frac{6\xi_j^2}{l_e^2}\right)\right],$$

$$k_{14} = \frac{12E(I_0 - I_{cj})}{l_e^3}\left[\frac{l_c^3}{l_e^2} + l_c\left(1 - \frac{5\xi_j}{l_e} + \frac{6\xi_j^2}{l_e^2}\right)\right],$$

$$k_{22} = \frac{12E(I_0 - I_{cj})}{l_e^2}\left[\frac{3l_c^3}{l_e^2} + 2l_c\left(\frac{3\xi_j}{l_e} - 2\right)^2\right],$$

$$k_{24} = \frac{12E(I_0 - I_{cj})}{l_e^2}\left[\frac{3l_c^3}{l_e^2} + 2l_c\left(2 - \frac{9\xi_j}{l_e} + \frac{9\xi_j^2}{l_e^2}\right)\right], \quad \text{and}$$

$$k_{44} = \frac{12E(I_0 - I_{cj})}{l_e^2}\left[\frac{3l_c^3}{l_e^2} + 2l_c\left(\frac{3\xi_j}{l_e} - 1\right)^2\right].$$

Similarly, the stiffness matrix $\mathbf{K}_{cj}$ can be constructed for other cracks. These element matrices are then assembled into the global stiffness matrix for the beam structure. Although free–free and cantilever beam structures are considered in the examples, these elements may be incorporated into beam elements of any complex structure.

2.3. ESTIMATION OF CRACK DEPTH AND LOCATION

The crack locations and depths are estimated using model updating. The penalty function method [17], based on natural frequencies only, is used. The vector of updating parameters is $\boldsymbol{\theta} = [x\ \mathrm{d}_c]^{\mathrm{T}}$, where $\mathbf{x} = [x_1, x_2, \ldots, x_p]$ and $\mathrm{d}_c = [d_{c1}, d_{c2}, \ldots, \mathrm{d}_{cp}]$ are the vectors of locations (measured from one end of the beam) of the p cracks and the corresponding crack depths. The measurement vector consists of the first m eigenvalues (natural frequency squared), $\mathbf{z}_e = [\lambda_{e1}, \lambda_{e2}, \ldots, \lambda_{em}]^{\mathrm{T}}$. The corresponding eigenvalues computed from the FE model are $\mathbf{z}_c = [\lambda_{c1}, \lambda_{c2}, \ldots, \lambda_{cm}]^{\mathrm{T}}$.

The eigenvalues may be written as a first order truncated Taylor series expansion in terms of the updating parameters, giving the error vector, $\boldsymbol{\varepsilon}$, as,

$$\boldsymbol{\varepsilon} = \delta\mathbf{z} - \mathbf{S}\delta\boldsymbol{\theta}, \tag{9}$$

where $\delta\boldsymbol{\theta}$ is the vector of perturbations in the updating parameters and $\delta\mathbf{z} = \mathbf{z}_e - \mathbf{z}_c$ is the eigenvalue error. It is important that the correct modes are paired, and this is conveniently checked using the modal assurance criteria (MAC) [48]. The sensitivity matrix, $\mathbf{S}$, is the first derivative of eigenvalues with respect to the updating parameters. These derivatives are readily computed [49] as

$$\frac{\partial \lambda_{ci}}{\partial x_j} = \boldsymbol{\phi}_i^{\mathrm{T}} \left[\frac{\partial \mathbf{K}}{\partial x_j} - \lambda_{ci} \frac{\partial \mathbf{M}}{\partial x_j} \right] \boldsymbol{\phi}_i \tag{10a}$$

and

$$\frac{\partial \lambda_{ci}}{\partial d_{cj}} = \boldsymbol{\phi}_i^{\mathrm{T}} \left[\frac{\partial \mathbf{K}}{\partial d_{cj}} - \lambda_{ci} \frac{\partial \mathbf{M}}{\partial d_{cj}} \right] \boldsymbol{\phi}_i, \tag{10b}$$

where $\boldsymbol{\phi}_i$ is the ith eigenvector. Since the effect of the cracks on the mass matrix is assumed to be negligible, the mass derivatives will be zero. The stiffness derivatives are computed by differentiating the system stiffness matrix. The position of the jth crack at the end of each iteration is given by x_j. Suppose that the jth crack is placed within the eth element of beam (see Figure 1), then

$$x_j = x(e) + \xi_j, \tag{11}$$

where $x(e)$ is the position of the eth node and ξ_j is the local co-ordinate of the jth crack in the eth element. Since $x(e)$ is fixed, $\partial \mathbf{K}/\partial x_j = \partial \mathbf{K}/\partial \xi_j$. Since the stiffness matrix due to the jth crack, $\mathbf{K}_{cj}$, is a continuous function of both ξ_j and, d_{cj}, the derivative may be computed analytically. From the expressions for the stiffness matrix, equation (8), it is clear that the stiffness matrix is a quadratic function of the crack position, ξ_j, and a linear function of the crack stiffness, EI_{cj}, which in turn is a cubic function of the crack depth, d_{cj}.

The penalty function, $\mathbf{J}$, is formed as [17]

$$\mathbf{J}(\delta\boldsymbol{\theta}) = \boldsymbol{\varepsilon}^{\mathrm{T}} \mathbf{W}_{\varepsilon} \boldsymbol{\varepsilon}, \tag{12}$$

where $\mathbf{W}_{\varepsilon}$ is the positive diagonal weighting matrix which reflects the confidence level in the frequency measurements. It is generally taken as the reciprocal of the variance (the square of the standard deviation) of the corresponding measurements [17]. It is implicit in equation (12) that the set of equations is over-determined, and so there are more measurements than parameters. Often the estimation is ill-conditioned, and in this case regularization can help [50, 51]. However, care must be exercised in identifying crack locations and depths where there is insufficient information in the measurements, and this may be conveniently checked by using the singular-value decomposition.

The estimated crack locations and their depths are obtained by minimizing $\mathbf{J}$ with respect to $\delta\boldsymbol{\theta}$, which involves differentiating $\mathbf{J}$ with respect to each parameter, and setting the result equal to zero. The perturbation in the parameter vector is then

$$\delta\boldsymbol{\theta} = [\mathbf{S}^{\mathrm{T}} \mathbf{W}_{\varepsilon} \mathbf{S}]^{-1} \mathbf{S}^{\mathrm{T}} \mathbf{W}_{\varepsilon}\, \delta\mathbf{z}. \tag{13}$$

Since equation (9) is a linear approximation, the method is iterative. A new model with the updated crack locations and their depths is generated, and the revised analytical eigenvalues and sensitivity matrix produced. The iteration process continues until the

solution converges. Since model updating minimizes a non-linear function using an iterative approach, a local rather than a global minimum may be found. This may be checked by using a number of different initial values for the unknown parameters.

3. VALIDATION OF THE CRACK MODEL

The expression for the effective length of the crack, l_c, given by equation (4) and also the triangular model for the stiffness reduction need to be validated. This section reports the experimental results from cantilever and free–free beams and compares these measurements to predictions from the model. The experimental modal tests were conducted on the beams with and without cracks, and the results compared to the corresponding predictions from the FE model. The experimental damage was implemented using saw cuts, and these correspond to open cracks.

3.1. CASE 1: AN ALUMINIUM CANTILEVER BEAM

The first example is an aluminium cantilever beam. Table 1 gives details of the geometric and material properties. The modal parameters of the beam were obtained by the impulse response method [52] using a small instrumented hammer for excitation and an accelerometer of mass 3·5 g for the response measurements. The experimental frequency response functions were processed through MATLAB-based modal analysis software to obtain the modal parameters. The modal test was conducted on the beam without any cracks and also with a single crack at 275 mm with the crack depth varying from 4 to 12 mm in steps of 4 mm. Table 2 gives the identified experimental natural frequencies.

An FE model of the cantilever beam was constructed using Euler–Bernoulli beam elements and including translational and rotational springs to simulate the boundary conditions at the clamped end of the beam. The FE model is shown schematically in Figure 4, and has 16 elements and 34 degrees of freedom. The stiffness of these boundary springs were tuned using the modal data of the uncracked beam to produce a validated FE model (see Table 2). The boundary stiffnesses, $k_t = 26{\cdot}5\,\text{MN/m}$ and $k_\theta = 150\,\text{kN m/rad}$, are required to simulate the translation and rotation flexibility of the clamped support. Using this FE model, the modal data of the cracked beam have been predicted, using the local

TABLE 1

The properties of the beams used for the experimental study

	Case 1	Case 2	Case 3
Boundary conditions	Cantilever	Free–free	Free–free
Material	Aluminium	Aluminium	Steel
Young's modulus, E	69·79 GN/m^2	69·79 GN/m^2	203·91 GN/m^2
Mass density, ρ	2600 kg/m^3	2600 kg/m^3	7800 kg/m^3
The Poisson Ratio, v	0·33	0·33	0·33
Beam length, L	996 mm	1832 mm	1330 mm
Beam width, w	50 mm	50 mm	25·30 mm
Beam depth, d	25 mm	25 mm	25·30 mm
Boundary stiffnesses	$k_t = 26{\cdot}5$ MN/m $k_0 = 150$ kN m/rad		

TABLE 2

The natural frequencies (Hz) *of the cantilever beam with one crack*

Mode	No crack			$d_{c1} = 4$ mm at $x_1 = 275$ mm			$d_{c1} = 8$ mm at $x_1 = 275$ mm			$d_{c1} = 12$ mm at $x_1 = 275$ mm		
	Experimental	Analytical	Error (%)	Experimental	Analytical	Error (%)	Experimental	Analytical	Error (%)	Experimental	Analytical	Error (%)
1	20·000	19·902	− 0·490	20·000	19·641	− 1·795	19·750	19·382	− 1·863	19·000	19·164	+ 0·863
2	124·500	124·543	+ 0·035	124·250	124·106	− 0·116	124·063	123·689	− 0·301	123·000	123·343	+ 0·279
3	342·188	345·507	+ 0·970	340·813	340·758	− 0·016	336·875	336·094	− 0·232	326·563	332·383	+ 1·780
4	664·375	664·317	− 0·009	662·813	663·020	+ 0·031	662·313	660·584	− 0·261	660·313	658·641	− 0·253

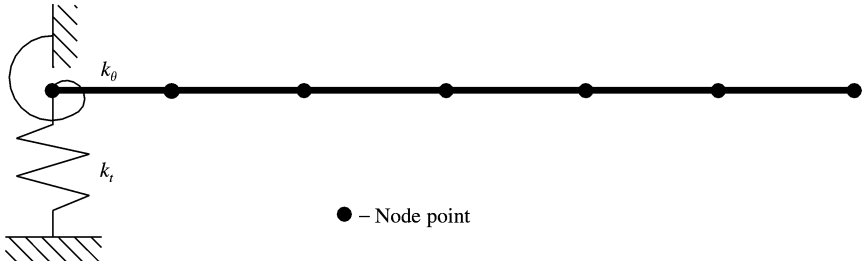

Figure 4. The FE model for the cantilever beam example.

flexibility (EI) of the beam element with a crack as proposed in section 2. Table 2 compares the measured and predicted natural frequencies for the cracked beam. The natural frequencies are estimated within an error of 1·9%.

3.2. CASE 2: AN ALUMINIUM FREE–FREE BEAM

The second example is a free–free aluminium beam whose physical dimensions and material properties are given in Table 1. Once again, the modal parameters of the beam were obtained using the impulse response method [52]. The modal tests were conducted on the beam without any cracks and with multi-cracks at different locations and crack depths. The experimentally identified natural frequencies are listed in Tables 3 and 4.

An FE model of the free–free beam was constructed using 27 Euler–Bernoulli beam elements and 56 degrees of freedom. The computed natural frequencies were close to the experimental results for the beam without any cracks. Tables 3 and 4 also show the experimental and predicted natural frequencies for the cracked beam. Once again, it was observed that the computed natural frequencies matched the experimental results closely and within an error of 1·5%.

3.3. CASE 3: A STEEL FREE–FREE BEAM

The third example is another free–free beam, but this time made of steel. Table 1 gives details of the physical dimensions and material properties for this beam. The free–free modal test was conducted on the beam without any cracks and with one crack at 430 mm, with the crack depth varying from 4 to 12 mm in steps of 4 mm. The experimentally identified natural frequencies are listed in Table 5, together with the predicted natural frequencies from an FE model with 20 elements and 42 degrees of freedom. Once again it was observed that the computed natural frequencies closely match the experimental results within 1·1%. The experimental and analytically computed natural frequencies of the cracked beam are compared in Table 5.

4. COMPARISON WITH OTHER CRACK MODELS

As indicated earlier, two simple crack models for beam structures have been used in earlier studies. The first approach is to assume the flexibility (EI) of the complete beam element with the crack being reduced. The second approach estimates the stiffness of the beam element with the crack by generating the flexibility matrix using an energy method

TABLE 3

The natural frequencies (Hz) *of the aluminium free–free beam with one crack*

Mode	No crack			$d_{c1} = 4$ mm at $x_1 = 595$ mm			$d_{c1} = 8$ mm at $x_1 = 595$ mm			$d_{c1} = 12$ mm at $x_1 = 595$ mm		
	Experimental	Analytical	Error (%)	Experimental	Analytical	Error (%)	Experimental	Analytical	Error (%)	Experimental	Analytical	Error (%)
1	40·000	39·789	− 0·527	39·688	39·379	− 0·778	39·375	39·094	− 0·714	39·063	38·857	− 0·527
2	109·688	109·680	− 0·007	109·063	108·206	− 0·786	108·125	107·132	− 0·918	105·938	106·278	+ 0·321
3	215·000	215·018	+ 0·008	215·000	214·087	− 0·425	214·688	213·825	− 0·402	214·375	213·622	− 0·351
4	355·000	355·440	+ 0·124	354·688	353·107	− 0·446	353·438	351·872	− 0·443	350·625	350·881	+ 0·073
5	528·750	530·977	+ 0·421	527·188	524·696	− 0·473	522·812	520·452	− 0·451	513·125	517·219	+ 0·798

TABLE 4

The natural frequencies (Hz) *of the aluminium free–free beam with two cracks*

Mode	No crack			$d_{c1} = 12$ mm at $x_1 = 595$ mm $d_{c2} = 4$ mm at $x_2 = 800$ mm			$d_{c1} = 12$ mm at $x_1 = 595$ mm $d_{c2} = 8$ mm at $x_2 = 800$ mm			$d_{c1} = 12$ mm at $x_1 = 595$ mm $d_{c2} = 12$ mm at $x_2 = 800$ mm		
	Experimental	Analytical	Error (%)	Experimental	Analytical	Error (%)	Experimental	Analytical	Error (%)	Experimental	Analytical	Error (%)
1	40·000	39·789	− 0·527	38·750	38·352	− 1·027	38·437	37·897	− 1·405	37·500	37·513	+ 0·035
2	109·688	109·680	− 0·007	105·938	105·890	− 0·045	105·938	105·510	− 0·404	105·625	105·559	− 0·062
3	215·000	215·018	+ 0·008	213·750	212·207	− 0·722	212·813	210·897	− 0·900	210·000	209·815	− 0·088
4	355·000	355·440	+ 0·124	350·000	348·920	− 0·308	349·063	347·235	− 0·524	345·625	345·876	+ 0·073
5	528·750	530·977	+ 0·421	512·500	514·575	+ 0·405	511·250	512·903	+ 0·323	507·500	510·560	+ 0·603

TABLE 5

The natural frequencies (Hz) *of the steel free–free beam with one crack*

Mode	*No crack*			$d_{c1} = 4$ mm at $x_1 = 430$ mm			$d_{c1} = 8$ mm at $x_1 = 430$ mm			$d_{c1} = 12$ mm at $x_1 = 430$ mm		
	Experimental	Analytical	Error (%)	Experimental	Analytical	Error (%)	Experimental	Analytical	Error (%)	Experimental	Analytical	Error (%)
1	75·313	75·171	− 0·188	74·688	74·406	− 0·377	74·063	73·628	− 0·587	72·813	72·958	+ 0·199
2	207·188	207·212	+ 0·012	205·625	204·183	− 0·701	202·500	201·283	− 0·601	197·188	198·928	+ 0·882
3	406·250	406·225	− 0·006	405·625	405·368	− 0·063	404·688	404·557	− 0·032	403·125	403·916	+ 0·196
4	667·813	671·536	+ 0·557	666·250	668·429	+ 0·327	662·813	665·356	+ 0·384	655·938	662·874	+ 1·057

[41]. The natural frequencies for the experimental examples above were computed by these two methods. The reduction in EI was estimated so that the computed natural frequencies were close to the experimental ones. The natural frequencies computed by these methods are listed in Tables 6–8, along with the frequencies predicted by the proposed method. The natural frequencies predicted by all of the methods are close to the experimental values. Although reducing EI is simple, it does not involve the size and location of the crack directly. The approach of Lee and Chung does involve both the size and location of the crack in the modelling, but the formulation is very complicated compared to the proposed method. Thus, the proposed method of crack modelling will be used for crack identification.

5. EXPERIMENTAL EXAMPLES OF CRACK IDENTIFICATION

To estimate the depth and location of a crack in a structure, the measured modal data and an initial estimate of the updating parameters are required. The measured data consisted of measured natural frequencies and mode shapes of the structure corresponding to the crack depth and location to be determined. This set of data is henceforth referred to as the target data for the iterative solution. The proposed crack model and estimation method for the detection of the crack depth and location has been assessed by applying the approach to the above experimental examples.

For all the three experimental examples, the detection of crack depth and location has been carried out by using the crack location x_1 and the crack depth d_{c1} as updating parameters. The first four measured natural frequencies were considered as the target data for this exercise and the weighting matrix was taken as the inverse of the target (measured) eigenvalues. Tables 9–11 give the results of the crack localization. Figure 5 shows the convergence history of crack depth and location for the cantilever beam, and is typical of the convergence for other examples. Of particular note is the fact that convergence is faster when the initial parameter estimates are closer to the updated estimates. The results show that the crack localization is very effective and the error in the estimated location and size is small. The crack location estimation is more accurate (error $<5\%$) compared to the crack depth (error $<30\%$). The higher error in the crack depth is partly due to the difficulties in measuring the crack depth experimentally, and partly due to the simple crack model used. However, the accuracy of the location is very encouraging, since this is usually quite difficult to estimate.

To test the performance of the approach when more than one crack is present, the depth and location of two cracks were estimated using the measured data from the aluminium free–free beam. The first five measured natural frequencies were used, since estimating four parameters with four measurements will always be sensitive to measurement noise and modelling error. Table 12 shows the result of the estimation. The errors are larger than for the one crack case, but this is because the same data were used to estimate twice as many parameters. Using five natural frequencies is insufficient to allow averaging of the noise and errors, and the results could be improved considerably by including more measured data (either higher natural frequencies, or possibly mode shapes). Even so the location is estimated with a typical accuracy of 5%, and is still under 10% in the worse case. Once again the estimates of the crack depth are poorer than the estimates of location. This is partly due to the reasons given for the one crack case, but also the opposite signs of the error is indicative of ill-conditioning in the estimation that would be improved by using a more measured data.

Of course the number of cracks present is not known initially. The normal approach is to identify a single crack, then identify multiple cracks, and assess the fit to the measured data

TABLE 6

Comparison of the natural frequencies (Hz) *of the cantilever beam with one crack estimated by different models*

	No crack		$d_{c1} = 4$ mm at $x_1 = 275$ mm				$d_{c1} = 8$ mm at $x_1 = 275$ mm				$d_{c1} = 12$ mm at $x_1 = 275$ mm			
Mode	Experimental	Analytical	Experimental	Reduced *EI*	Lee *et al.* [41]	Proposed method	Experimental	Reduced *EI*	Lee *et al.* [41]	Proposed method	Experimental	Reduce *EI*	Lee *et al.* [41]	Proposed method
1	20·000	19·902	20·000	19·753	19·822	19·641	19·750	19·543	19·580	19·382	19·000	19·251	19·048	19·164
2	124·500	124·543	124·250	124·289	124·410	124·106	124·063	123·934	124·008	123·689	123·000	123·446	123·147	123·343
3	342·188	345·508	340·813	342·571	343·920	340·758	336·875	338·591	339·263	336·094	326·563	333·366	329·937	332·383
4	664·375	664·317	662·813	662·782	663·539	663·020	662·313	660·732	661·299	660·584	660·313	658·087	656·975	658·641

TABLE 7

The natural frequencies (Hz) *of the aluminium free–free beam with one crack estimated by different models*

	No crack		$d_{c1} = 4$ mm at $x_1 = 275$ mm				$d_{c1} = 8$ mm at $x_1 = 275$ mm				$d_{c1} = 12$ mm at $x_1 = 275$ mm			
Mode	Experimental	Analytical	Experimental	Reduced *EI*	Lee *et al.* [41]	Proposed method	Experimental	Reduced *EI*	Lee *et al.* [41]	Proposed method	Experimental	Reduce *EI*	Lee *et al.* [41]	Proposed method
1	40·000	39·789	39·688	39·594	39·698	39·379	39·375	39·371	39·415	39·094	39·063	39·021	38·77	38·857
2	109·688	109·680	109·063	108·899	109·311	108·206	108·125	108·036	108·200	107·132	105·938	106·735	105·850	106·278
3	215·000	215·018	215·000	214·815	214·927	214·087	214·688	214·592	214·654	213·825	214·375	214·258	214·085	213·622
4	355·000	355·440	354·688	354·549	355·028	353·107	353·438	353·559	353·783	351·872	350·625	352·059	351·136	350·881
5	528·750	530·977	527·188	527·603	529·363	524·696	522·812	524·011	524·684	520·452	513·125	518·843	515·507	517·219

TABLE 8

The natural frequencies of the steel free–free beam with one crack estimated by different models

	No crack		$d_{c1} = 4$ mm at $x_1 = 430$ mm				$d_{c1} = 8$ mm at $x_1 = 430$ mm				$d_{c1} = 12$ mm at $x_1 = 430$ mm			
Mode	Experimental	Analytical	Experimental	Reduced *EI*	Lee *et al.* [41]	Proposed method	Experimental	Reduced *EI*	Lee *et al.* [41]	Proposed method	Experimental	Reduced *EI*	Lee *et al.* [41]	Proposed method
1	75·313	75·171	74·688	74·670	74·938	74·406	74·063	74·004	74·224	73·628	72·813	72·284	72·634	72·958
2	207·188	207·212	205·625	205·190	206·262	204·183	202·500	202·630	203·458	201·283	197·188	198·278	197·764	198·928
3	406·250	406·225	405·625	405·642	405·974	405·368	404·688	404·907	405·235	404·557	403·125	403·672	403·770	403·916
4	667·813	671·536	666·250	669·335	670·550	668·429	662·813	666·527	667·615	665·356	655·938	661·720	661·635	662·874

TABLE 9

The crack depth and location estimation for the cantilever beam example (*initial parameter estimates*: $x_1 = 400\,\text{mm}$, $d_{c1} = 2\,\text{mm}$)

		No crack	Case 1a		Case 1b		Case 1c	
			Actual (target)	Estimated (% error)	Actual (target)	Estimated (% error)	Actual (target)	Estimated (% error)
Crack location	x_1 (mm)	—	275·00	272·29 (−0·985)	275·00	276·60 (+0·582)	275·00	288·27 (+4·825)
Crack depth	d_{c1} (mm)	—	4·00	3·65 (−8·750)	8·00	7·063 (−11·712)	12·00	15·49 (+29·08)
		Experiment	Experiment	Predicted	Experiment	Predicted	Experiment	Predicted
Natural frequency (Hz)	1	20·000	20·000	19·662	19·750	19·444	19·000	19·095
	2	124·500	124·250	124·169	124·063	123·757	123·000	122·752
	3	342·188	340·813	341·233	336·875	337·113	326·563	330·548
	4	664·375	662·813	663·048	662·313	661·318	660·313	660·861
Number of iterations required			05		07		15	

TABLE 10

The crack depth and location estimation for the aluminium free–free beam example (*initial parameter estimates*: $x_1 = 832\,\text{mm}$, $d_{c1} = 2\,\text{mm}$)

		No crack	Case 2a		Case 2b		Case 2c	
			Actual (target)	Estimated (% error)	Actual (target)	Estimated (% error)	Actual (target)	Estimated (% error)
Crack location	x_1 (mm)	—	595·00	581·30 (−2·302)	595·00	600·33 (+0·896)	595·00	594·56 (−0·074)
Crack depth	d_{c1} (mm)	—	4·00	3·07 (−23·250)	8·00	7·082 (−12·475)	12·00	11·687 (−2·608)
		Experiment	Experiment	Predicted	Experiment	Predicted	Experiment	Predicted
Natural frequency (Hz)	1	40·000	39·688	39·499	39·375	39·341	39·063	38·874
	2	109·688	109·063	108·650	108·125	108·074	105·938	106·330
	3	215·000	215·000	214·175	214·688	214·076	214·375	213·625
	4	355·000	354·688	353·673	353·438	352·894	350·625	350·973
Number of iterations required			12		08		11	

TABLE 11

The crack depth and location estimation for the steel free–free beam example (initial parameter estimates: $x_1 = 630\,\text{mm}$, $d_{c1} = 2\,\text{mm}$)

		No crack	Case 3a		Case 3b		Case 3c	
			Actual (target)	Estimated (% error)	Actual (target)	Estimated (% error)	Actual (target)	Estimated (% error)
Crack location	x_1 (mm)	—	430·00	438·10 (+1·884)	430·00	443·02 (+3·028)	430·00	436·60 (+1·535)
Crack depth	d_{c1} (mm)	—	4·00	3·664 (−8·40)	8·00	7·70 (−3·75)	12·00	15·000 (+25·00)
		Experiment	Experiment	Predicted	Experiment	Predicted	Experiment	Predicted
Natural frequency (Hz)	1	75·313	74·688	74·456	74·063	73·650	72·813	72·545
	2	207·188	205·625	204·552	202·500	201·955	197·188	197·997
	3	406·250	405·625	405·694	404·688	405·366	403·125	404·238
	4	667·813	666·250	668·006	662·813	663·693	655·938	659·771
Number of iterations required			15		12		07	

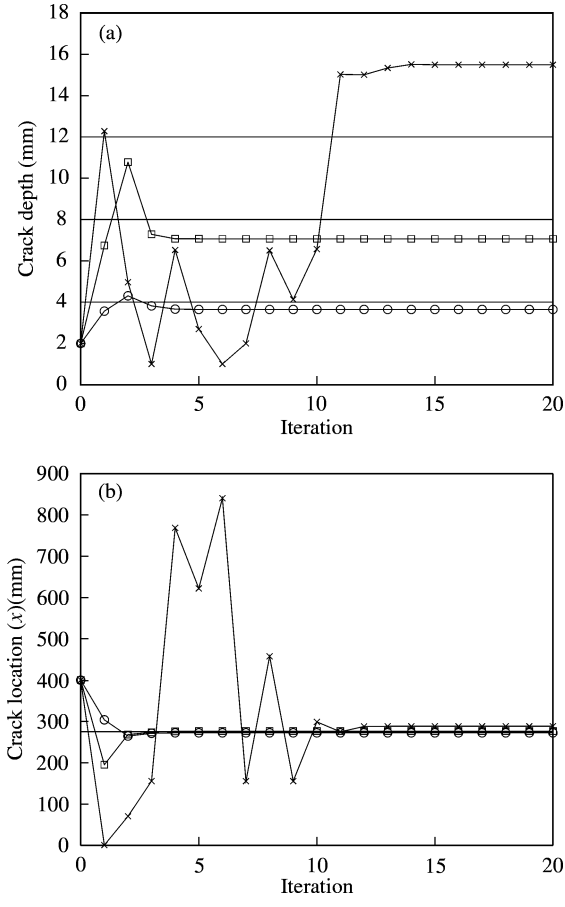

Figure 5. The convergence of the estimated crack depth and location for the cantilever beam: (a) Depth estimation; (b) Location estimation: ——, target; ○, case 1a; □, Case 1b; and ×, Case 1c.

for significant improvement. Suppose that only one crack is present, but an attempt is made to identify the location and depth of two cracks. Table 13 shows the results of this exercise for the aluminium free–free beam example. A lower limit of 0·1 mm has been placed on the crack depth to eliminate possible numerical problems near zero crack depth. It is clear that in all cases one of the two identified cracks has a negligible effect (approximately zero depth), and the position of the other crack is identified accurately. Again, the location is estimated more accurately than the crack depth.

The model updating process is iterative because the cost function that is minimized (the error in the eigenvalues) is a highly non-linear function of the parameters. To illustrate this non-linearity, Figure 6 shows surface plots of the percentage frequency error (root mean square of percentage frequencies errors) versus crack location and depth for experimental cases 1b and 2c. It may be seen that there is one predominant minimum for case 1b and two minima symmetrically placed along the length of the beam for case 2c. The two local minima for case 2c indicate the symmetrical configuration of the free–free beam and the estimation process may converge to either of the minima. This limitation should be acceptable for a symmetric structure, and if necessary the mode shapes may be used to distinguish between the minima. However for an unsymmetrical structure (case 1b), there is

TABLE 12

The estimation of the depth and location of two cracks for the aluminium free–free beam example (*initial parameter estimates*: $x_1 = 400\,\text{mm}$, $d_{c1} = 1\,\text{mm}$, $x_2 = 1000\,\text{mm}$, $d_{c2} = 1\,\text{mm}$)

		No crack	Case 4a		Case 4b		Case 4c	
			Actual (target)	Estimated (% error)	Actual (target)	Estimated (% error)	Actual (target)	Estimated (% error)
Crack location	x_1 (mm)	—	595·00	595·72 (+0·121)	595·00	614·48 (+3·274)	595·00	627·46 (+5·455)
	x_2 (mm)	—	800·00	824·91 (+3·114)	800·00	878·73 (+9·841)	800·00	849·60 (+6·20)
Crack depth	d_{c1} (mm)	—	12·00	13·24 (+10·333)	12·00	15·13 (+26·083)	12·00	17·50 (+45·833)
	d_{c2} (mm)	—	4·00	2·77 (−30·75)	8·00	4·51 (−41·625)	12·00	8·82 (−26·50)
		Experiment	Experiment	Predicted	Experiment	Predicted	Experiment	Predicted
Natural frequency (Hz)	1	40·000	38·750	38·491	38·437	38·163	37·500	37·544
	2	109·688	105·938	105·93	105·938	105·93	105·625	105·80
	3	215·000	213·750	212·54	212·813	211·66	210·000	210·11
	4	355·000	350·000	349·57	349·063	348·67	345·625	346·44
	5	528·750	512·500	515·34	511·250	512·09	507·500	508·26
Number of iterations required			15		11		12	

TABLE 13

The estimation of the depth and location of two cracks for the aluminium free–free beam example, when only one crack is present (initial parameter estimates: $x_1 = 400\,\text{mm}$, $d_{c1} = 1\,\text{mm}$, $x_2 = 1000\,\text{mm}$, $d_{c2} = 1\,\text{mm}$)

		No crack	Case 2a		Case 2b		Case 2c	
			Actual (target)	Estimated (% error)	Actual (target)	Estimated (% error)	Actual (target)	Estimated (% error)
Crack location	x_1 (mm)	—	595·00	562·45 (−5·47%)	595·00	578·68 (−2·74%)	595·00	583·90 (−1·87%)
	x_2 (mm)	—	—	332·00	—	332·00	—	332·00
Crack depth	d_{c1} (mm)	—	4·00	2·48 (−38·00%)	8·00	5·50 (−31·25%)	12·00	13·00 (+8·33%)
	d_{c2} (mm)	—	—	0·10	—	0·10	—	0·10
Natural frequency (Hz)	1	40·000	39·688	39·51	39·375	39·28	39·063	38·82
	2	109·688	109·063	108·59	108·125	107·67	105·938	105·90
	3	215·000	215·000	213·92	214·688	213·68	214·375	213·18
	4	355·000	354·688	353·96	353·438	353·03	350·625	351·28
	5	528·750	527·188	526·44	522·812	522·54	513·125	515·69
Number of iterations required			8		18		22	

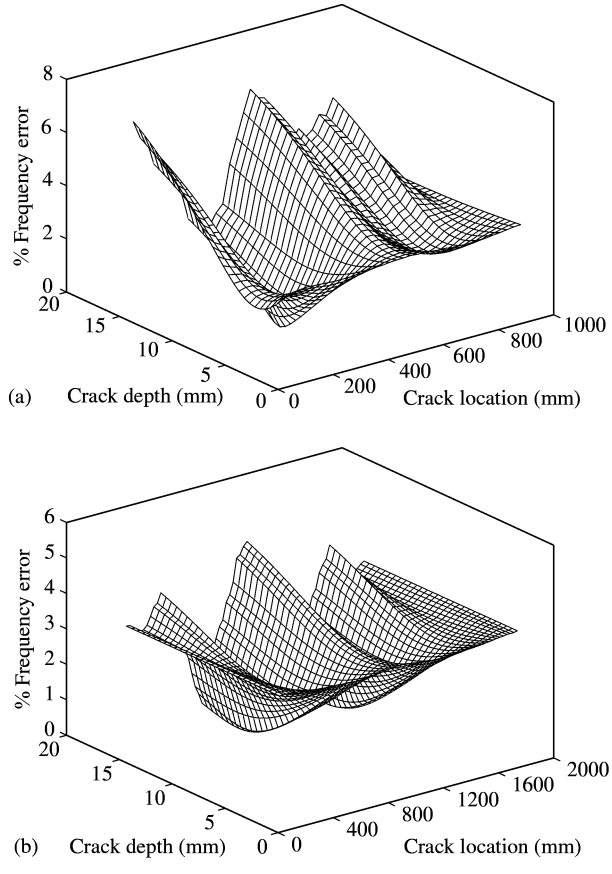

Figure 6. The percentage natural frequency error as a function of crack depth and location.

only one global minimum and this indicates the uniqueness of the identified parameters. It is also clear that local minima exist, and multiple initial parameter values should be taken to ensure that the global minimum is obtained.

6. CONCLUDING REMARKS

A non-intrusive and non-destructive method for the estimation of both the location and the depth of cracks in beam-type structures, by the solution of an inverse vibration problem, has been presented. The methodology uses a baseline FE model along with the modal test data in a gradient-based model updating method. The changes in the natural frequencies of the structure due to the presence of a crack are used. Methods of modelling of beam-type structures with multi-cracks, as well as their identification (both crack size and location), have been discussed. The validation of the proposed method has been demonstrated with three simple experimental examples. It has also been observed from experimental examples that the estimation of the crack location is more accurate than the estimation of the crack depth. In considering the application of the proposed technique to real problems, the

accurate location of a crack is more important for predictive and preventive maintenance than its exact size. Beam models have been used in the development of the method, although a similar approach for two- and three-dimensional components is possible.

ACKNOWLEDGMENTS

Jyoti K. Sinha acknowledges the support of the Department of Science and Technology of India through the award of a BOYSCAST Fellowship. Sinha also acknowledges his parent organization, B.A.R.C., India, for their consistent support and encouragement. Michael Friswell acknowledges the support of the EPSRC through the award of an Advanced Fellowship.

REFERENCES

1. S. W. Doebling, C. R. Farrar and M. B. Prime 1998 *Shock and Vibration Digest* **30**, 91–105. A summary review of vibration-based damage identification methods.
2. P. Cawley and R. D. Adams 1979 *Journal of Strain Analysis* **14**, 49–57. The locations of defects in structures from measurements of natural frequencies.
3. M. I. Friswell, J. E. T. Penny and D. A. L. Wilson 1994 *Modal Analysis*: *The International Journal of Analytical and Experimental Modal Analysis* **9**, 239–254. Using vibration data and statistical measures to locate damage in structures.
4. J. E. T. Penny, D. A. L. Wilson and M. I. Friswell 1993 *IMAC* XI, 861–867. Damage location in structures using vibration data.
5. M. H. Richardson and M. A. Mannan 1992 *IMAC* X, 502–507. Remote detection and location of structural faults using modal parameters.
6. Y. Narkis 1994 *Journal of Sound and Vibration* **172**, 549–558. Identification of crack location in vibrating simply supported beams.
7. T. Wolff and M. Richardson 1989 *IMAC* VII, 87–94. Fault detection in structures from changes in their modal parameters.
8. A. K. Pandey, M. Biswas and M. M. Samman 1991 *Journal of Sound and Vibration* **145**, 321–332. Damage detection from change in curvature mode shapes.
9. C. H. J. Fox 1992 *IMAC* X, 522–528. The location of defects in structures: a comparison of the use of natural frequency and mode shape data.
10. J. H. Kim, H. S. Jeon and C. W. Lee 1992 *IMAC* X, 536–540. Application of the modal assurance criteria for detecting and locating structural faults.
11. C. P. Ratcliffe 1997 *Journal of Sound and Vibration* **204**, 505–517. Damage detection using a modified Laplacian opeartor on mode shape data.
12. P. F. Rizos, N. Aspragathos and A. D. Dimarogonas 1990 *Journal of Sound and Vibration* **138**, 381–388. Identification of crack location and magnitude in a cantilever beam.
13. A. K. Pandey and M. Biswas 1994 *Journal of Sound and Vibration* **169**, 3–17. Damage detection in structures using change in flexibility.
14. S. W. Doebling, L. D. Peterson and K. F. Alvin 1996 *American Institute of Aeronautics and Astronautics Journal* **34**, 1678–1685. Estimation of reciprocal residual flexibility from experimental modal data.
15. T. W. Lim 1991 *American Institute of Aeronautics and Astronautics Journal* **29**, 2271–2274. Structural damage detection using modal test data.
16. O. S. Salawu 1997 *Engineering Structures* **19**, 718–723. Detection of structural damage through changes in frequencies: a review.
17. M. I. Friswell and J. E. Mottershead 1995 *Finite Element Model Updating in Structural Dynamics*. Dordrecht: Kluwer Academic Publishers.
18. J. M. Ricles and J. B. Kosmatka 1992 *American Institute of Aeronautics and Astronautics Journal* **30**, 2310–2316. Damage detection in elastic structures using vibratory residual forces and weighted sensitivity.
19. C. Farhat and F. M. Hemez 1993 *American Institute of Aeronautics and Astronautics Journal* **31**, 1702–1711. Updating of FE dynamic models using an element by element sensitivity methodology.

20. F. M. HEMEZ and C. FARHAT 1995 *Modal Analysis*: *The International Journal of Analytical and Experimental Modal Analysis* **10**, 152–166. Structural damage detection via a finite element model updating methodology.
21. J. K. SINHA and M. I. FRISWELL 2001 *Journal of Sound and Vibration* **244**, 137–153. The location of spring supports from measured vibration data.
22. M. I. FRISWELL and J. E. MOTTERSHEAD 2001 *DAMAS* 2001: 4*th International Conference on Damage Assessment of Structures*, *Cardiff*, 201–210. Inverse methods in structural health monitoring.
23. I. TRENDAFILOVA 2001 *DAMAS* 2001: 4*th International Conference on Damage Assessment of Structures*, *Cardiff*, 85–93. Pattern recognition methods for damage diagnosis in structures from vibration measurements.
24. K. WORDEN, G. MANSON and N. R. FIELLER 1999 *Journal of Sound and Vibration* **229**, 647–667. Damage detection using outlier analysis.
25. F.-K. CHANG (Editor) 1999 *Structural Health Monitoring* 2000. Technomic Publishing Co. Lancaster, Pennsylvania, U.S.A. *Proceedings of the second International Workshop on Structural Health Monitoring*, *Stanford University*, *Stanford*, *CA*.
26. W. J. STASZEWSKI 2000 *The International Journal of Systems Science* **11**, 1381–1396. Advanced data pre-processing for damage identification based on pattern recognition.
27. A. D. DIMAROGONAS 1996 *Engineering Fracture Mechanics* **55**, 831–857. Vibration of cracked structures: a state of the art review.
28. W. OSTACHOWICZ and M. KRAWCZUK 2001 *DAMAS* 2001: 4*th International Conference on Damage Assessment of Structures*, *Cardiff*, 185–199. On modelling of structural stiffness loss due to damage.
29. O. S. SALAWU and C. WILLIAMS 1993 *IMAC* XI, 254–260. Structural damage detection using experimental modal analysis — a comparison of some methods.
30. M. M. F. YUEN 1985 *Journal of Sound and Vibration* **103**, 301–310. A numerical study of the eigen parameters of a damaged cantilever beam.
31. T. D. CHAUDHARI and S. K. MAITI 2000 *International Journal of Solids and Structures* **37**, 761–779. A study of vibration of geometically segmented beams with and without crack.
32. M. BOLTEZAR, B. STRANCAR and A. KUHELJ 1998 *Journal of Sound and Vibration* **211**, 729–734. Identification of transverse crack location in flexural vibrations of free-free beams.
33. F. ISMAIL, A, IBRAHIM and H. R. MARTIN 1990 *Journal of Sound and Vibration* **140**, 305–317. Identification of fatigue cracks from vibration testing.
34. J. FERNANDEZ-SAEZ, L. RUBIO and C. NAVARRO 1999 *Journal of Sound and Vibration* **225**, 345–352. Approximate calculation of the fundamental frequency for bending vibrations of cracked beams.
35. M. W. OSTACHOWICZ and M. KRAWCZUK 1991 *Journal of Sound and Vibration* **150**, 191–201. Analysis of the effect of cracks on the natural frequencies of a cantilever beam.
36. M. H. H. SHEN and J. E. TAYLOR 1991 *Journal of Sound and Vibration* **150**, 457–484. An identification problem for vibrating cracked beams.
37. E. I. SHIFRIN and R. RUOTOLO 1999 *Journal of Sound and Vibration* **222**, 409–423. Natural frequencies of a beam with an arbitrary number of cracks.
38. M.-H. H. SHEN and C. PIERRE 1990 *Journal of Sound and Vibration* **138**, 115–134. Natural modes of Bernoulli–Euler beam with symmetric cracks.
39. K. LAKSHMI NARAYAN and C. JEBARAJ 1999 *Journal of Sound and Vibration* **228**, 977–994. Sensitivity analysis of local/global modal parameters for identification of a crack in a beam.
40. M. KRAWCZUK and W. M. OSTACHOWICZ 1993 *Finite Element in Analysis and Design* **13**, 225–235. Hexahedral finite element with an open crack.
41. Y.-S. LEE and M.-J. CHUNG 2000 *Computers and Structures* **77**, 327–342. A study on crack detection using eigenfrequency test data.
42. J. A. BRANDON 1998 *Proceedings of the Institution of Mechanical Engineers Part C*: *Journal of Mechanical Engineering Science* **212**, 441–454. Some insights into the dynamics of defective structures.
43. M. KISA and J. A. BRANDON 2000 *Journal of Sound and Vibration* **238**, 1–18. The effects of closure of cracks on the dynamics of a cracked cantilever beam.
44. S. CHRISTIDES and A. D. S. BARR 1984 *International Journal of Mechanical Science* **26**, 639–648. One dimensional theory of cracked Bernoulli–Euler beams.
45. M. M. ABDEL WAHAB, G. DE ROECK and B. PEETERS 1999 *Journal of Sound and Vibration* **228**, 717–730. Parameterization of damage in reinforced concrete structures using model updating.

46. M.-H. H. SHEN and C. PIERRE 1994 *Journal of Sound and Vibration* **170**, 237–259. Free vibrations of beams with a single edge crack.
47. S. H. S. CARNEIRO and D. J. INMAN 2001 *Journal of Sound and Vibration* **244**, 729–737. Comments on the free vibrations of beams with a single-edge crack.
48. R. J. ALLEMANG and D. L. BROWN 1982 *IMAC* I, 110–116. A correlation coefficient for modal vector analysis.
49. R. L. FOX and M. P. KAPOOR 1968 *American Institute of Aeronautics and Astronautics Journal* **6**, 2426–2429. Rates of change of eigenvalues and eigenvectors.
50. M. I. FRISWELL, J. E. MOTTERSHEAD and H. AHMADIAN 2001 *Proceedings of the Royal Society of London, Series A*: *Mathematical, Physical and Engineering Sciences* **359**, 169–186. Finite element model updating using experimental test data: parameterisation and regularisation.
51. M. I. FRISWELL, J. E. T. PENNY and S. D. GARVEY 1997 *Inverse Problems in Engineering* **5**, 189–215. Parameter subset selection in damage location.
52. D. J. EWINS 1984 *Modal Testing*: *Theory and Practice*, Research Studies Press. Taunton, Somerset, U.K.